

According to the X-ray analysis, the blackish micro-matter are composed of micro-quartz particles, less than silt-size in diameter, and clay minerals, such as kaolinite and montmorillonite.

The origin of these inorganic fine particles is estimated as follows.

- (1) Decomposition, solution and outflowing from the Kaolin-beds over geologic time.
- (2) Washing out of the existing abandoned open pits during heavy rain.
- (3) Decomposition, solution and outflowing of interstitial packing clay minerals, altered minerals and iron oxide and so on, of the grains of quartz and feldspar composing the arenitic red sandstone and arkose sandstone beds, which are the geologic components of the basin.
- (4) The secondary fine particles produced by the re-dissection process of the alluvial deposits of the plain.

As for the blackish color, carbonization of remains and/or gleyzation of subsurface soil layer are considerable, but the reasons for these are not apparent.

5.4 Reference Data on Supplied Debris Quantity

Soil erosion is controlled by many factors such as the latitude of the area, the climate, the precipitation and its intensity, the geology, the landform, the soil type, the vegetation cover, and the level of human socioeconomic activity and so on.

Accordingly, it is quite difficult to pursue an average annual quantity of erosion.

Fluvial transportation load is a weighty index, showing the rate of erosion in the basin.

Attempts to measure the annual quantity of surface erosion and the annual denudation depth have been made since long ago, but discussion and data on these problems are unavoidably rough and variable and are only sufficient in estimating general tendencies of regional erosion.

An example is shown in Fig. S5.5.1 and Table S5.5.1, S5.5.2.

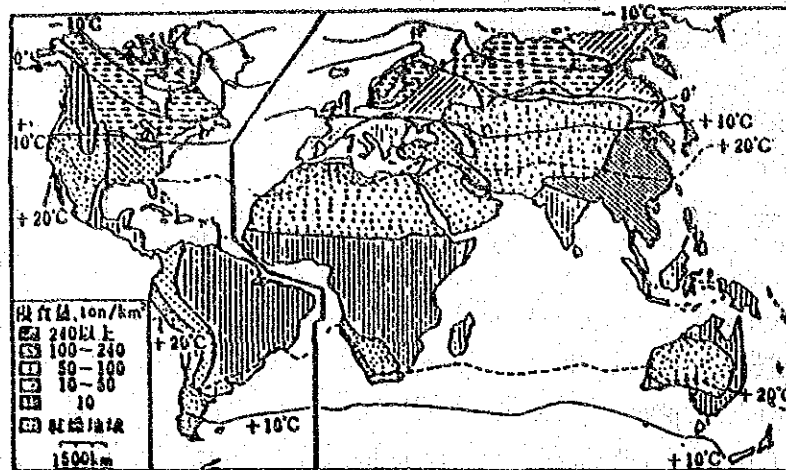


Fig. S5.5.1 Map on Surface Erosion Distribution

data from "Potamorphology" TAKAYAMA, S., 1975

Table S5.5.1 Rivers of the World and Their Annual Sediment Load over 10⁸ton/year

Name of River	Name of Country	Catchment Area 10 ⁴ Km ²	Annual Sediment Load 10 ⁸ ton	Specific Sediment Load ton/Km ²
The Yellow river	China	67.3	20.8	3,090
The Ganges	India	95.5	16.0	1,675
The Yangtze River	China	194.1	5.5	283
The Indus	Pakistan	96.9	4.8	495
The Amazon	Brazil	578.0	4.0	69
The Mississippi	U.S.A	322.1	3.4	105
The Irrawaddy	Burma	43.0	3.3	767
The Missouri	U.S.A	137.0	2.4	175
The Mekong	Thailand	79.5	1.9	238
The Colorado	U.S.A	63.7	1.5	235
The Red	Vietnam	11.9	1.4	1,176
The Nile	Egypt	298.0	1.2	40

Table S5.5.2 Annual Sediment Load from the Continents

Name of Continent	Area 10 ⁴ km ²	Sediment Load 10 ⁸ ton
North America	2,073	19.6
South America	1,941	12.0
Africa	1,993	5.4
Australia	518	3.3
Europe	932	3.2
Asia	2,692	159.1
Total	10,149	201.6

According to Fig. S5.5.1, Paraguay belongs to the zone of $50 \sim 100 \text{ ton/km}^2/\text{y} = 0.5 \sim 1.0 \text{ ton/ha/year}$

after 「 MILOSHOLY, EROSION AND ENVIRONMENT 」

original Translated by S. Okamura & Haruyama 1980

Regarding soil erosion by surface run-off on slopes, some observed values are shown in Tables S5.5.3, S5.5.4 and S5.5.5.

Table S5.5.3 Effects of Gradient on Soil Loss by Bennet

Soil Type and Locality	Observ. period (year)	Precipitation (mm)	Length (m)	Gradient (m)	Crop	Soil Loss (t/ha)
Silty Loam Ohio	9	965	22.1	8.0	corn	158.8
				12.0		222.4
				20.0		243.7
Fine Loam Texas	10	1,032	22.1	8.7	cotton	50.1
	8	1,092		16.5		136.8
Loam Missouri	14	1,025	22.1	3.7	corn	44.1
	10	749		8.0		114.0

Table S5.5.4 Effects of Slope Length on Soil Loss by Bennet

Soil type and locality	Observation period (year)	Precipitation (mm)	Crop	Length (m)	Gradient (%)	Soil loss (t/ha)
Silty Loam Iowa	1933 - 35	684	corn	48.0	8	28.9
				96.0		40.3
				192.0		52.6
Fine Loam Oklahoma	1931 - 36	800	cotton	11.0	7.7	42.5
				22.1		55.6
				44.3		99.3
Fine Loam Texas	1931 - 36	1,038	cotton	11.0	8.7	45.9
				22.1		68.9
				44.3		107.7
Silty Loam Wisconsin	1933 - 36	820	corn	11.0	16	159.0
				22.1		248.0
				44.3		286.6
Silty Loam Montana	1934 - 35	851	corn	20.4	10	56.8
				54.9		133.7
				82.2		164.0

Table S5.5.5 Effects of Cultivation Method on Soil Loss by Cherkasov

Arrangement of ridge	Amount of Soil Loss (t/ha)
Contour line method	1.7
Slope of gradient 4.4%	12.2
Slope of gradient 16%	27.2

The above-mentioned data on farmland shows very deviated values depending on the observation conditions regarding all the factors of gradient, slope length and cultivating methods and makes it very difficult to decide on the allowable rate of soil erosion in farmland.

According to the measurement at a test site composed of forested fresh soil in the U.S.A., the normal soil loss ranges in rate from 0.25 to 1.48t/ha/year, which corresponds to the rate of natural soil genesis.

In the U.S.A, the allowable rate of erosion ranges from 2.5 to

12.5t/ha/year.

In Czechoslovakia, the allowable rate of erosion for the shallow soil layer (<30cm) is 1t/ha/year, that of the (30~60cm) layer is 4t/ha/year and that of the 60~120cm deep layer is 10t/ha/year.

However, it is well known that the forest plays a very important role in the preservation of soil. In recent years the washing-out of the surface soil layer and the desertification accompanying over cutting of tropical forests has become a global problem.

The effect of vegetation cover is well indicated by the experimentation carried out in Tanzania, East Africa by a group of Swedish researchers. Measured amounts of soil loss after a rain in each type of environment : forest, grassland, millet farm and the bare ground of the same area, with a gradient of 3.5%, are as follows (Fig. S5.5.2).

	Run-off coefficient	Amounts of soil loss (t/ha)
Forest	0.4	0
Grassland	1.9	0
Millet farm	26.0	78.1
Bare land	50.4	146.3

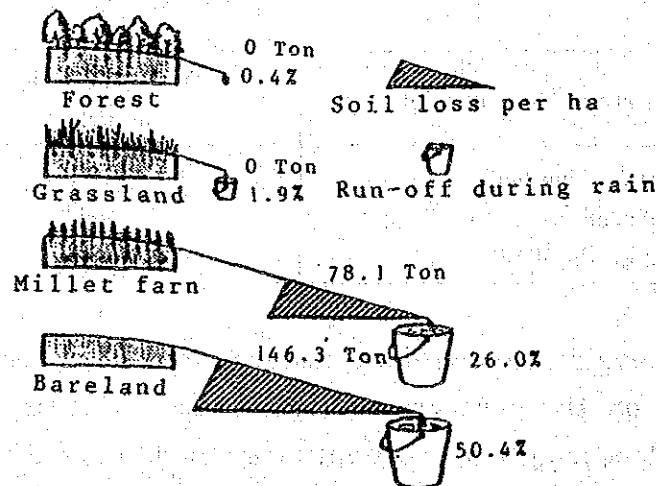


Fig.S5.5.2 Accelerating Soil Erosion by Loss of Vegetation Cover

after [Earth Environment Report]

H.ISHI

In a supposing sense the above experimental value will be applied to the Lake Ypacarai basin.

The inflowing area of the lake (now temporally limited to the Pirayu basin and both the east and the west sides of the Lake) is almost 500Km². Supposing that the amount of soil loss is 40t/ha, which is the medium value of grassland and millet farm, after the same scale rain as during the experiment (amount of precipitation is obscure), 2,000,000tons of soil (about 1,200,000m³, at a specific gravity of 1.7) will be washed out. Actually, a more reduced amount of soil will be expected because of the expanded gently sloped grassland.

As an example, the results of observation and experimentation carried out in Okinawa Island in Japan at a small basin which is composed mainly of lateritic soil (red soil) of Paleozoic beds origin and is located on a pineapple hill slope, are shown in Table S5.5.6.

Taken from "Report on Control and Counter
Measure Plan for Outwashing of the Red Soil"

Okinawa Development Agency

Table S5.5.6 Amount of Outwashing of Red Soil after Rainfall per Unit Area

	m ³ /Km ²					
Date of Rain	82.8.23	10.28	11.29	12.21	83.8.26	9.25
Amount of Soil Loss	260.0mm	115.0	90.5	53.0	168.0	98
Area I 6.55Km ²	69.5	9.1	20.6	3.4	4.0	21.6
Area II 7.24Km ²	83.6	7.3	19.2	1.6	2.6	29.8

In this small basin (13.8Km²) composed of by Area I and II, a value amount of 8,400m³/year (608.6m³/Km²/y) was obtained.

This is converted to 10.3t/ha/y, at specific gravity of 1.7.

In supposing that all pineapple farmland in this basin has a gradient of 15%, the experimental formula shows the amount of outwashed soil of

577t/ha. Supposing that all slopes were regulated at a gradient under 5%, the formula shows greatly decreased amounts at $143.3\text{m}^3/\text{Km}^2$ (2.4t/ha).

In all cases, it is clearly shown that the degree of vegetation cover and the gradient of land will have notable effects on the outwashing of soil.

Tentatively, the past amounts of erosion in the Lake Ypacarai basin are estimated as follows.

Though the mechanism and/or period of formation of the Lake are unsolved, considering the geologic time scale, total amounts of produced and transported debris achieve huge quantities. Namely, it is equivalent to the volume equal to the depression of graben-like land form, and also the eroded volume from the older mountains up to the present gently undulating hills.

According to a very bold rough estimation, the eroded mountain volume based on the topographic profile within the limits of 550Km^2 (excluding the Yuquyry basin and the Salado basin), is indicated at amounts of about $1.5\sim 2 \times 10^{11}\text{m}^3$, and is incredible at the scale and/or gradient of the present basin.

As mentioned above, although the beginning age of this land form formation is obscure, supposing boldly that the erosion process had been started in the late Cretaceous or early Tertiary age, which are estimated to have been under violent geotectonic movement and occurred about 70 million years ago, and continues up to present, the following value is obtained.

$$\begin{aligned} 1.5 \times 10^{11} \text{m}^3 / 7 \times 10^7 \text{year} / 550 \text{km}^2 &= 3.9 \text{m}^3 / \text{km}^2 / \text{year} \\ &= 6.6 \text{ton} / \text{km}^2 / \text{year} \\ &= 0.066 \text{t} / \text{ha} / \text{year} \end{aligned}$$

This value is unexpectedly smaller than that of Okinawa Island. Although the above estimation is almost meaningless due to the fact that it is based on mostly supposition, it was tried in order to get closer to the degree of erosion.

CHAPTER VI

FUTURE STUDIES

6.1 Reliability of Estimated Numerical Value

Water quality surveys on water pollution are scarce. Thus, this report has relied, to a large part, on on-site investigation and a few surveys due to the lack of available data.

Therefore, it is believed that there will be many areas within this data that will require revision.

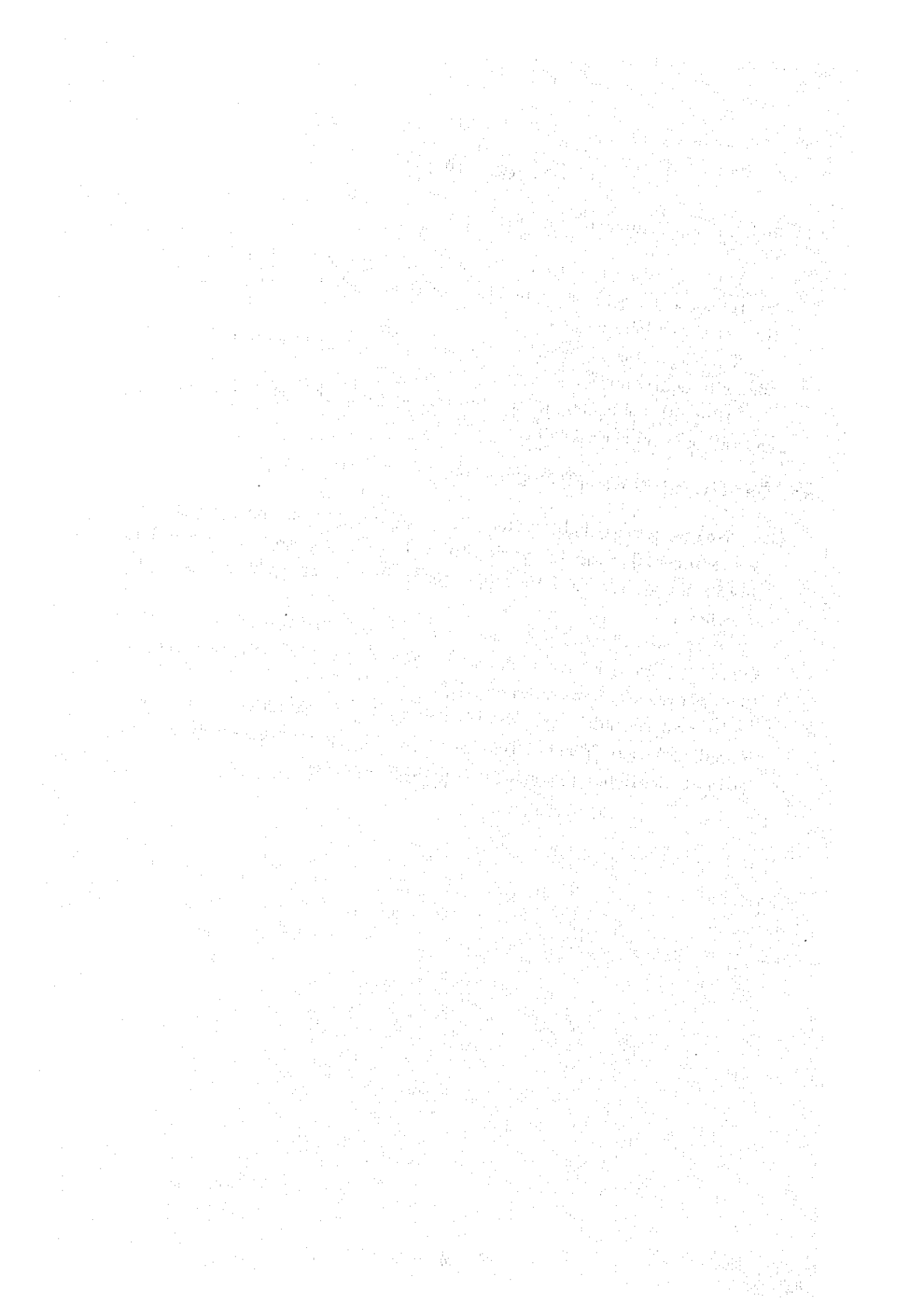
After all, for benefit in the future, much importance is attached to indication by numerical values.

6.2 On the Origin of Water Pollution

No area of remarkable water pollution discharge was found in the basin. At the time of flooding, the SS density in the inflowing rivers increases, but this is not a characteristic phenomenon in a basin as it can be seen anywhere.

It is generally known that SS, during flood, for the most part, settles around the mouth of rivers. This is recognized by the rise of the riverbed in the lower reaches of the inflowing river.

It is appropriate to state that the origin of water pollution in the lake is from the lake itself and not from the basin, judging from the situation of the basin. This will be a theme to prove in future studies.



FIGURES

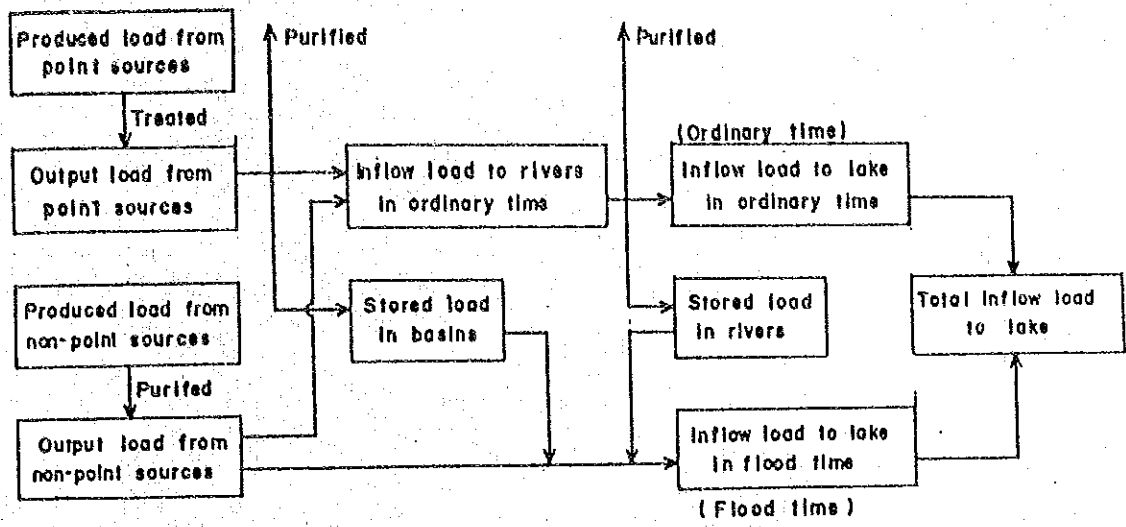


FIG. S5.1.1(a) INFLOW PROCESS OF POLLUTION LOAD

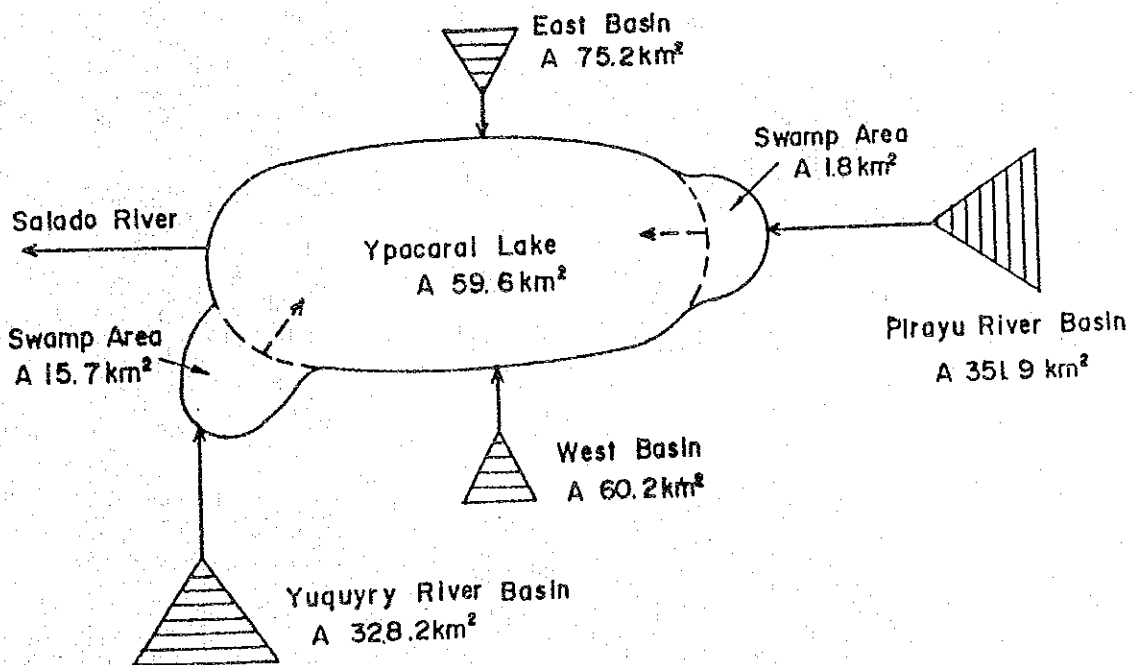


FIG. S5.1.1(b) INFLOW MODEL OF POLLUTION LOAD

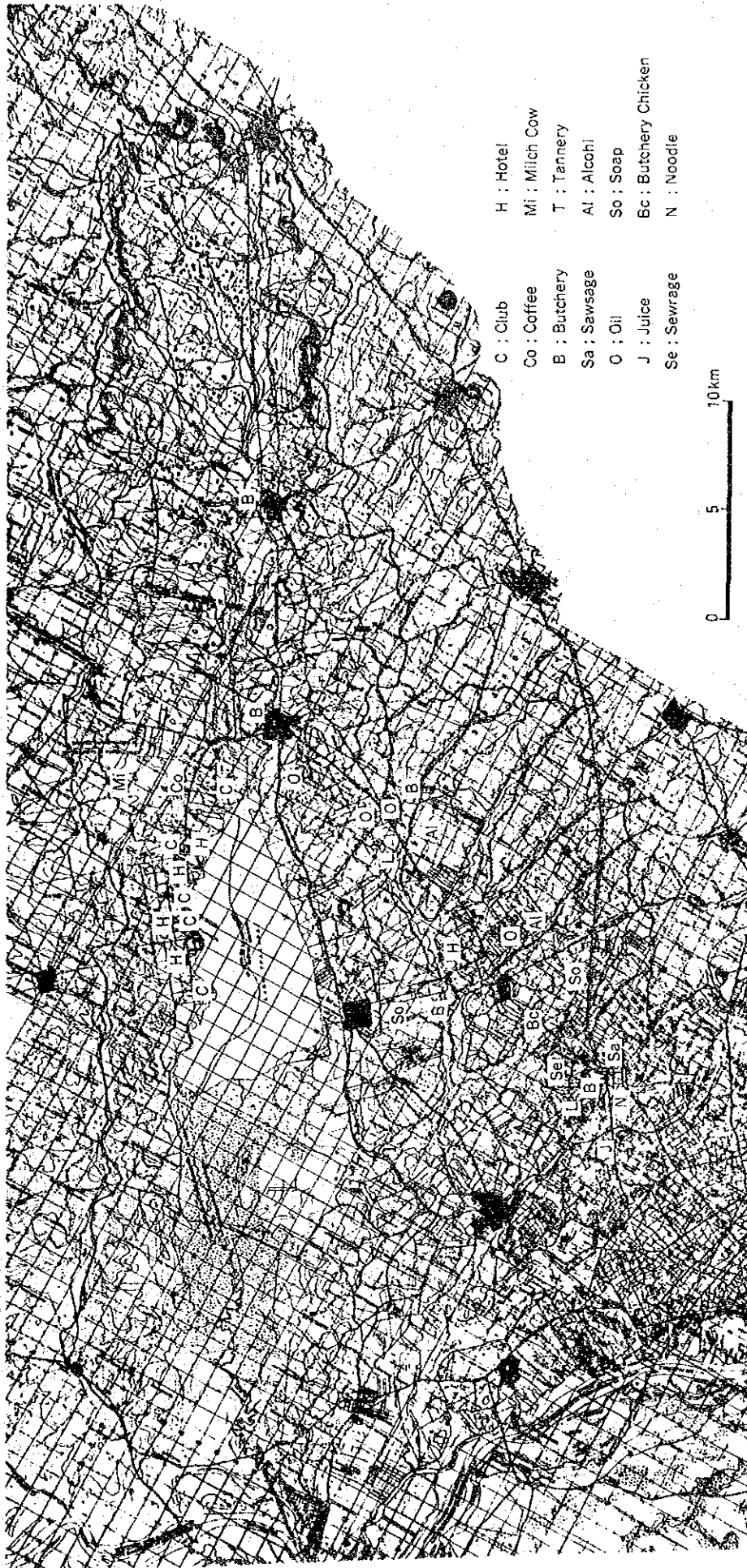
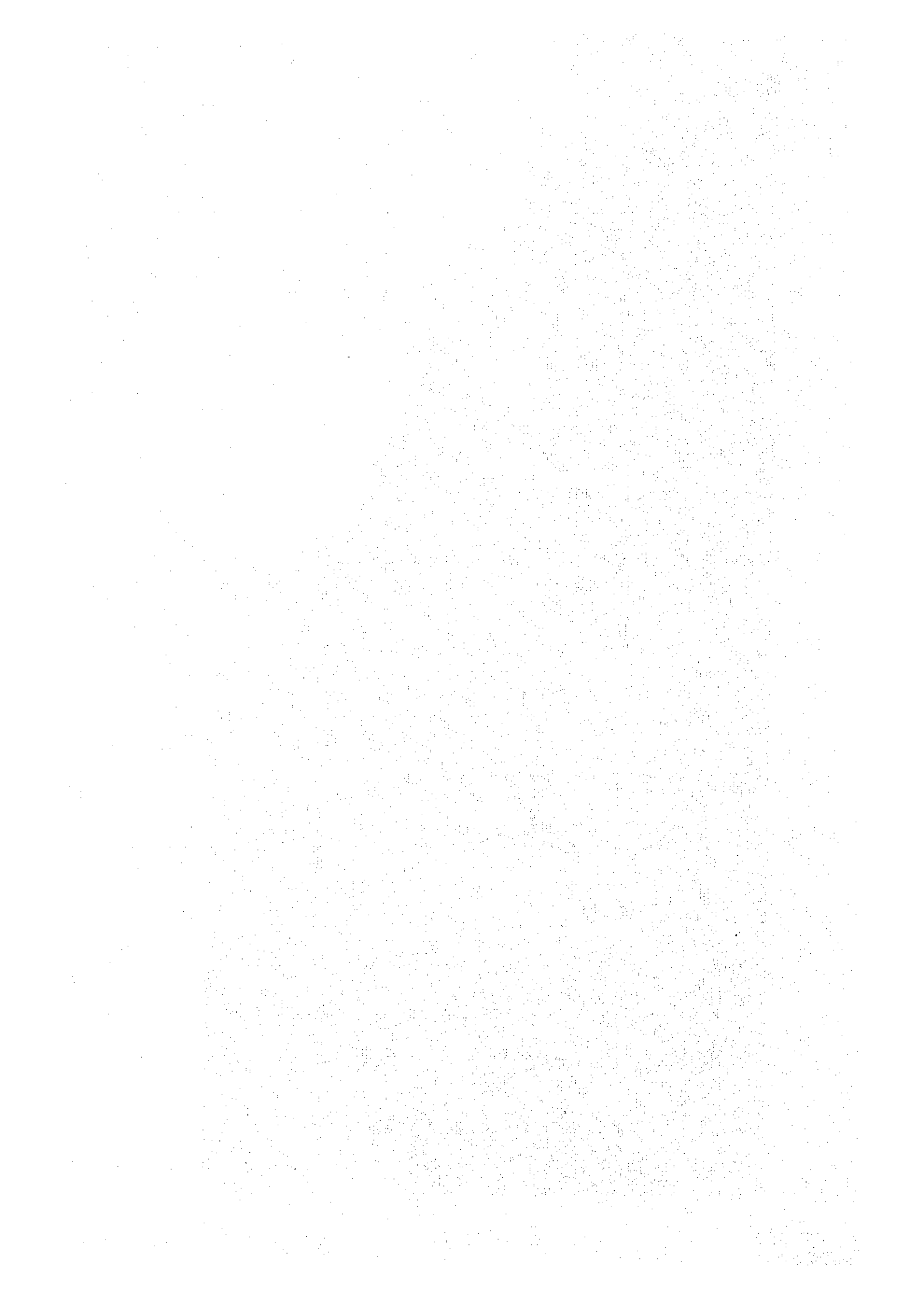


Fig. S5.1.1.2 Location of Main Point Pollution Sources



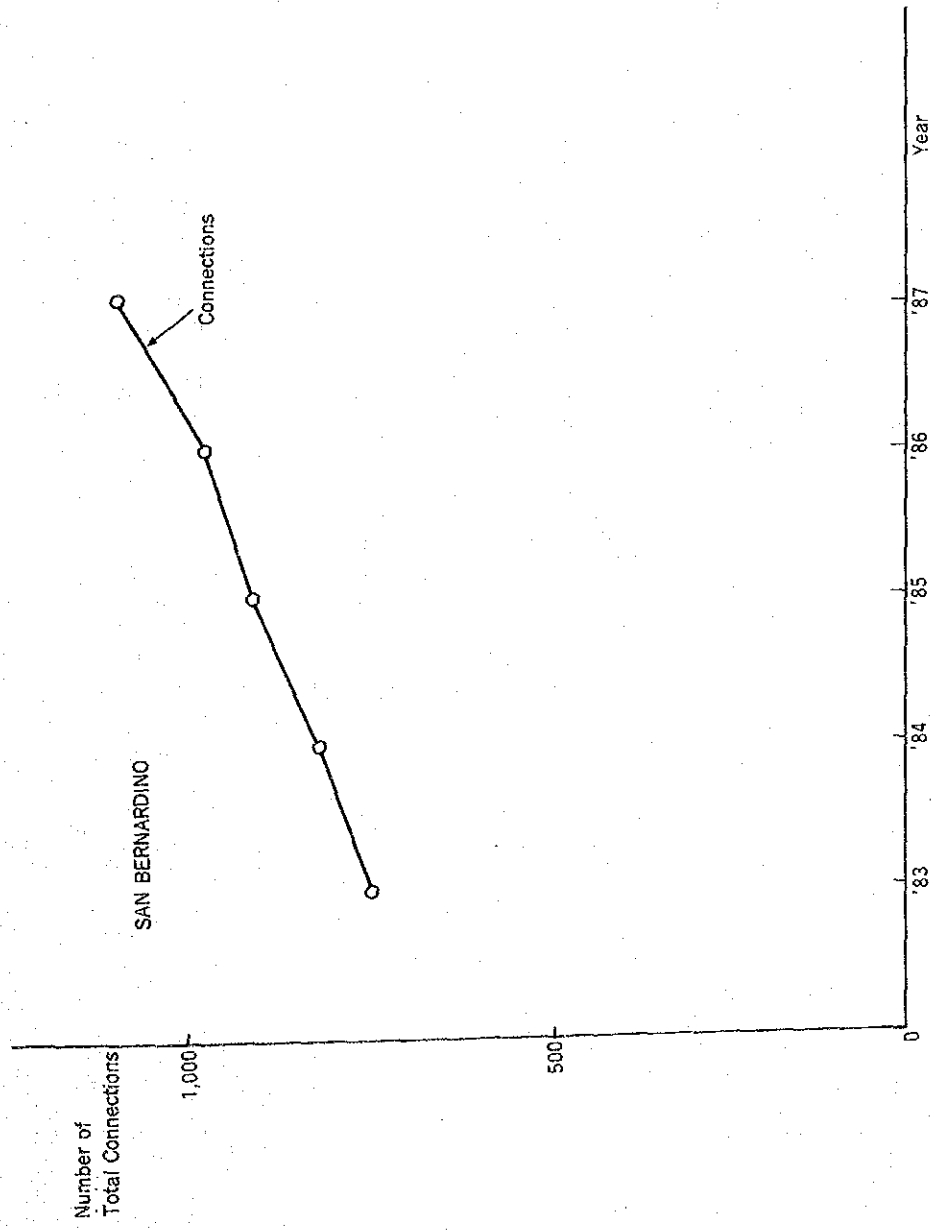


Fig.S5.2.1.Variation of Purified Water Consumption from Operational Data by CORPOSANA in SAN BER.

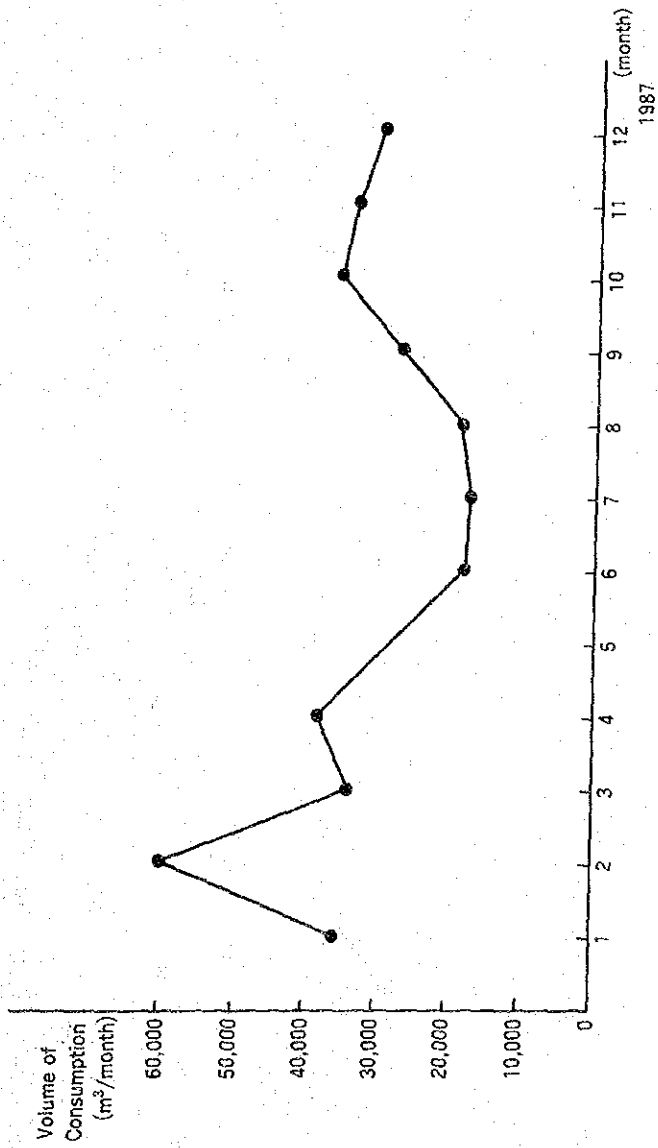


Fig.S5.2.2 Seasonal Variation of Purified Water Consumption from Operation Data by CORPOSANA in SAN BER.

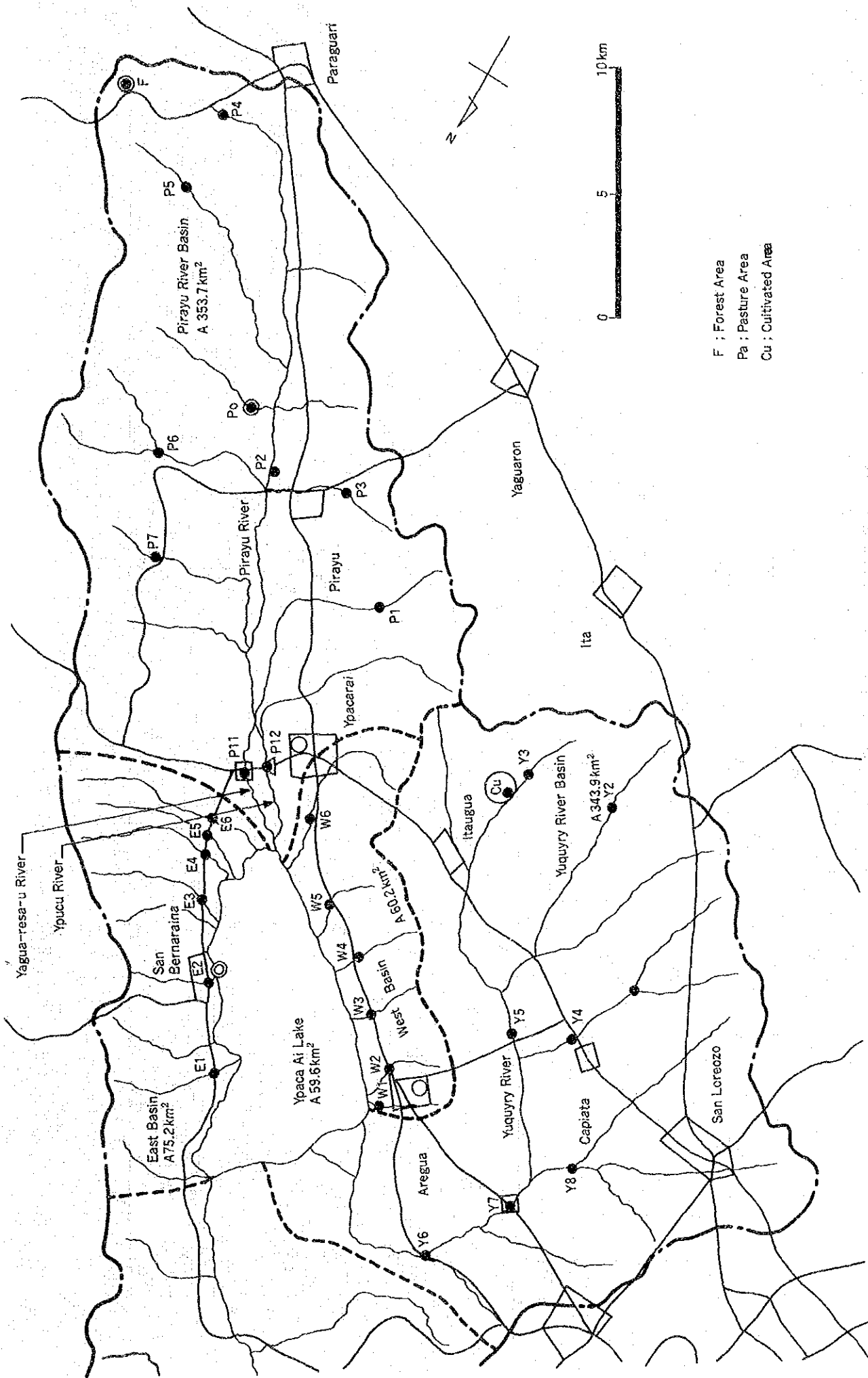
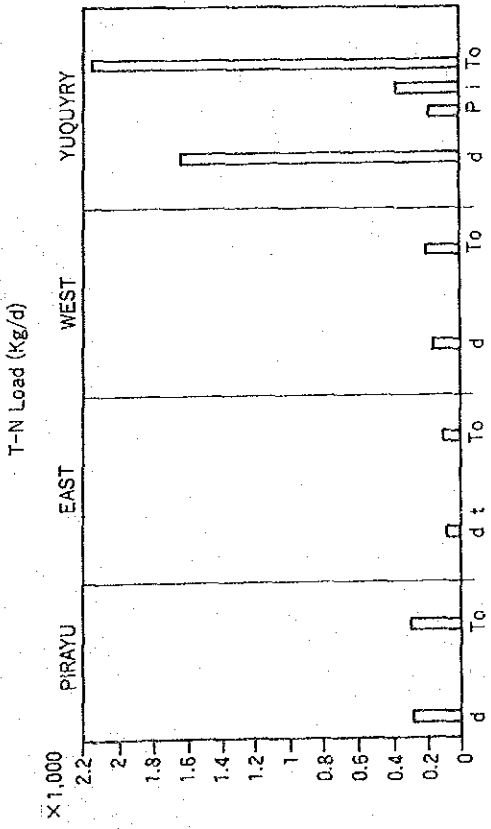
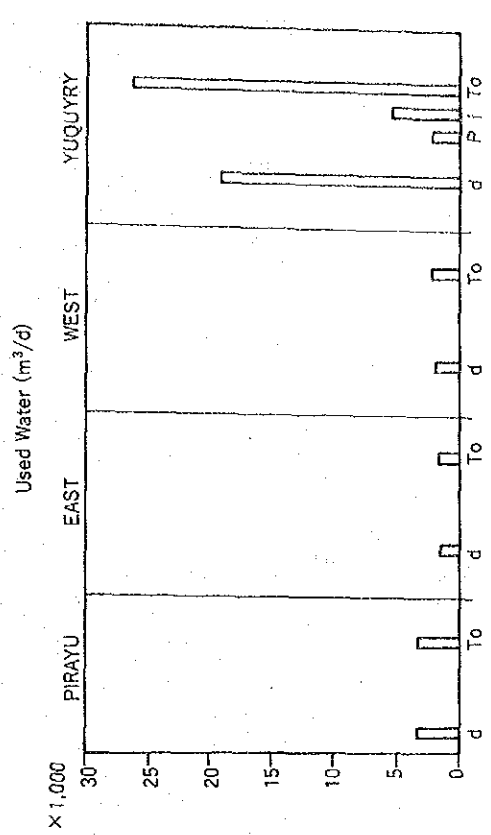
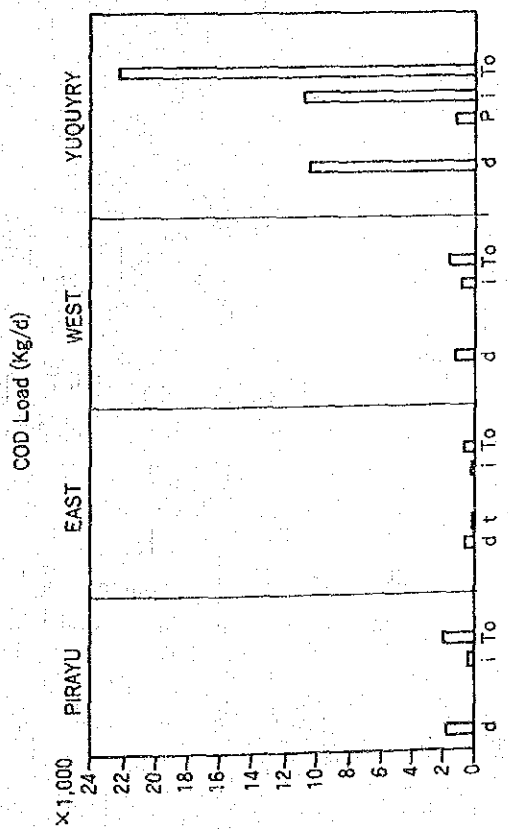
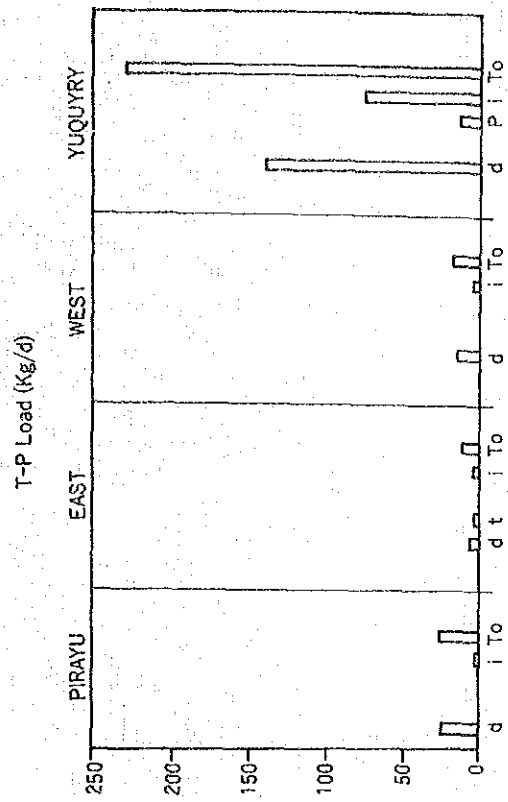
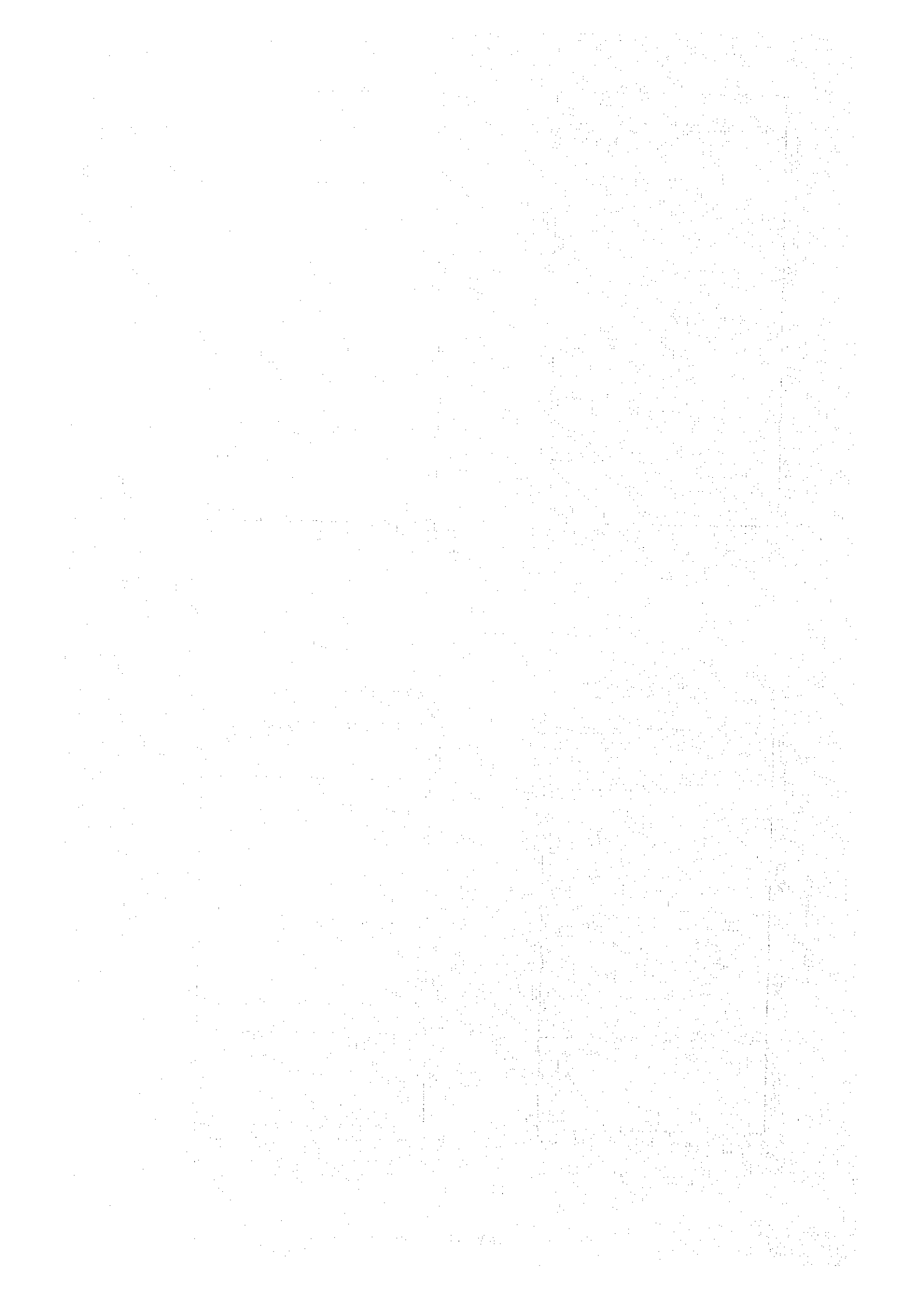


Fig. S5.2.3 Location of Survey Points



d ; Domestic p ; Public
t ; Hotel & Club i ; Industry
To ; Total

Fig S5.3.1 Generated Loading of Point-Pollution-Sources



PIRAYU B.

YUQUYRY B.

△ Survey Point at River

$\frac{Q(m^2/S)}{L(kg/d)}$ COD

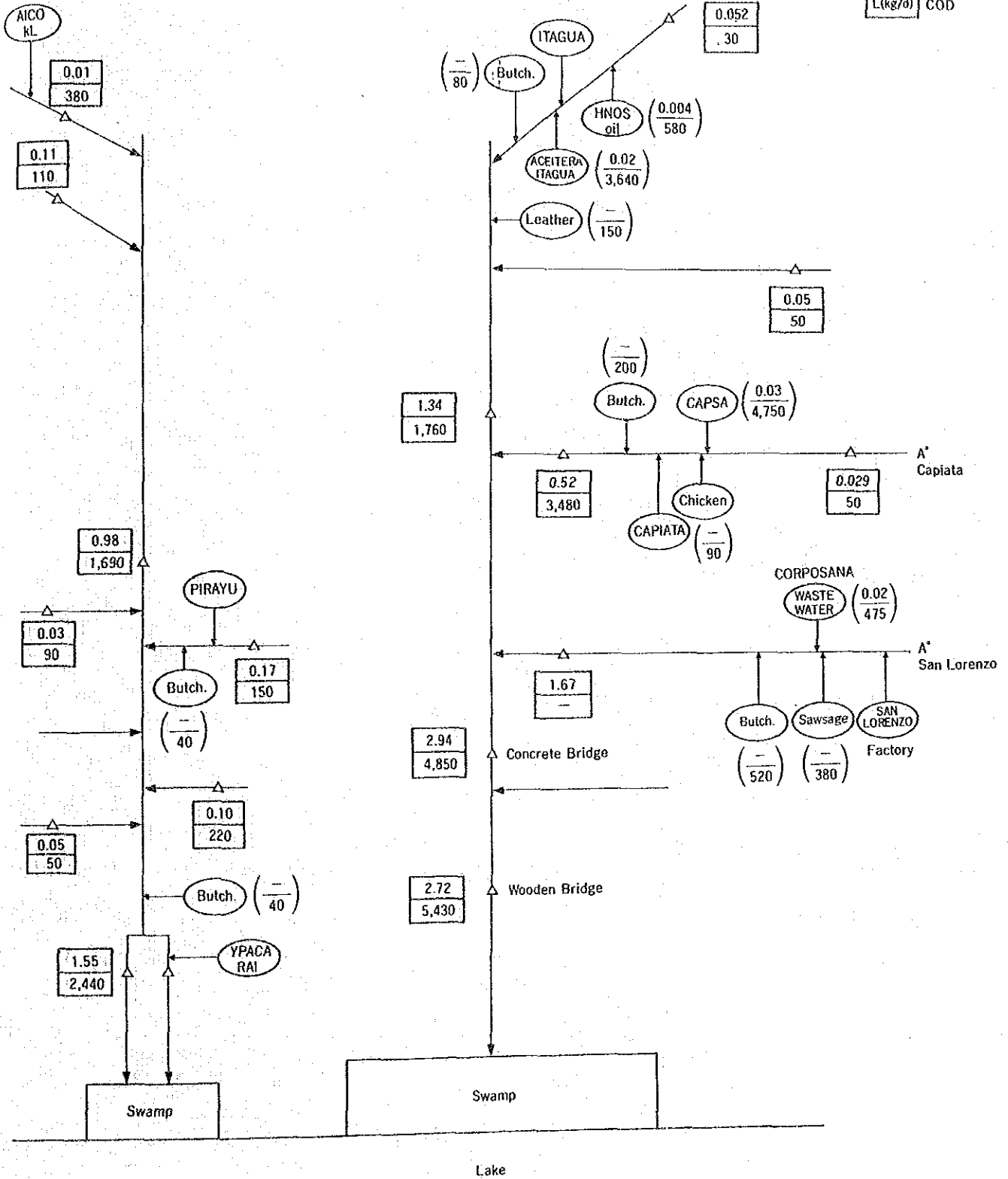
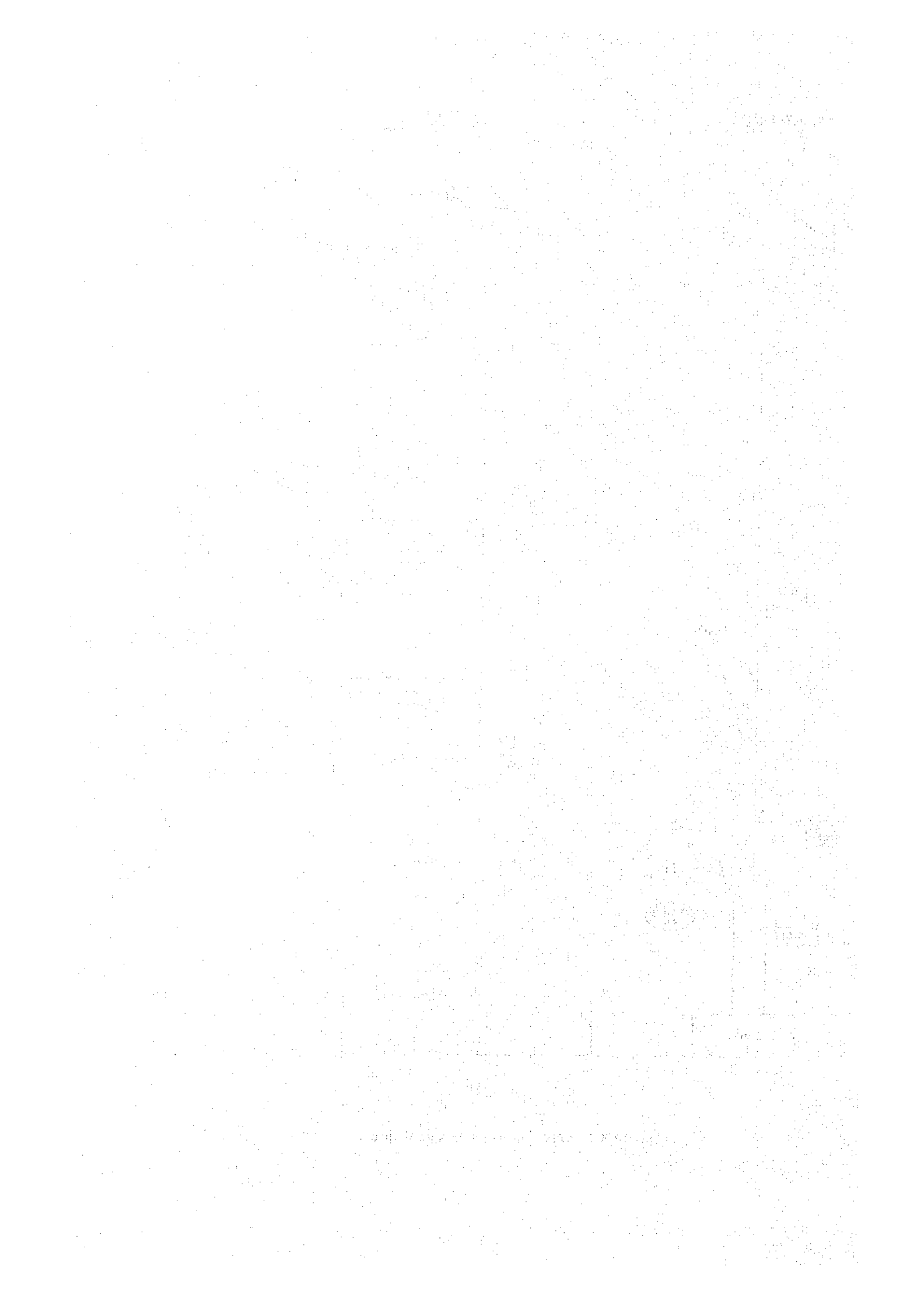


Fig. S5.3.2 COD Inflow Load in Normal Time

1988. 7



PIRAYU B.

YUQUYRY B.

△ Survey Point at River

$Q(m^3/s)$
 $L(kg/d)$ SS

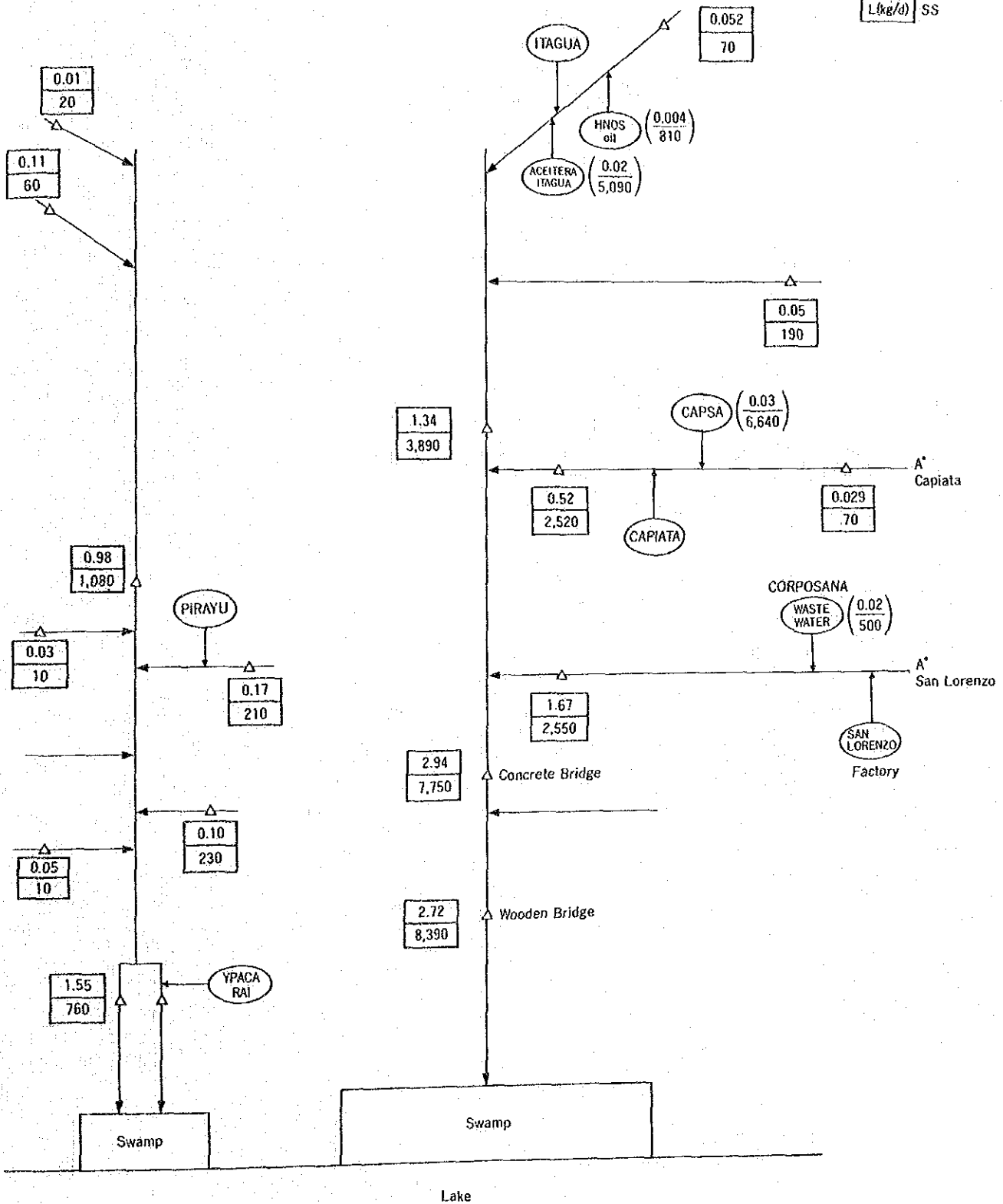
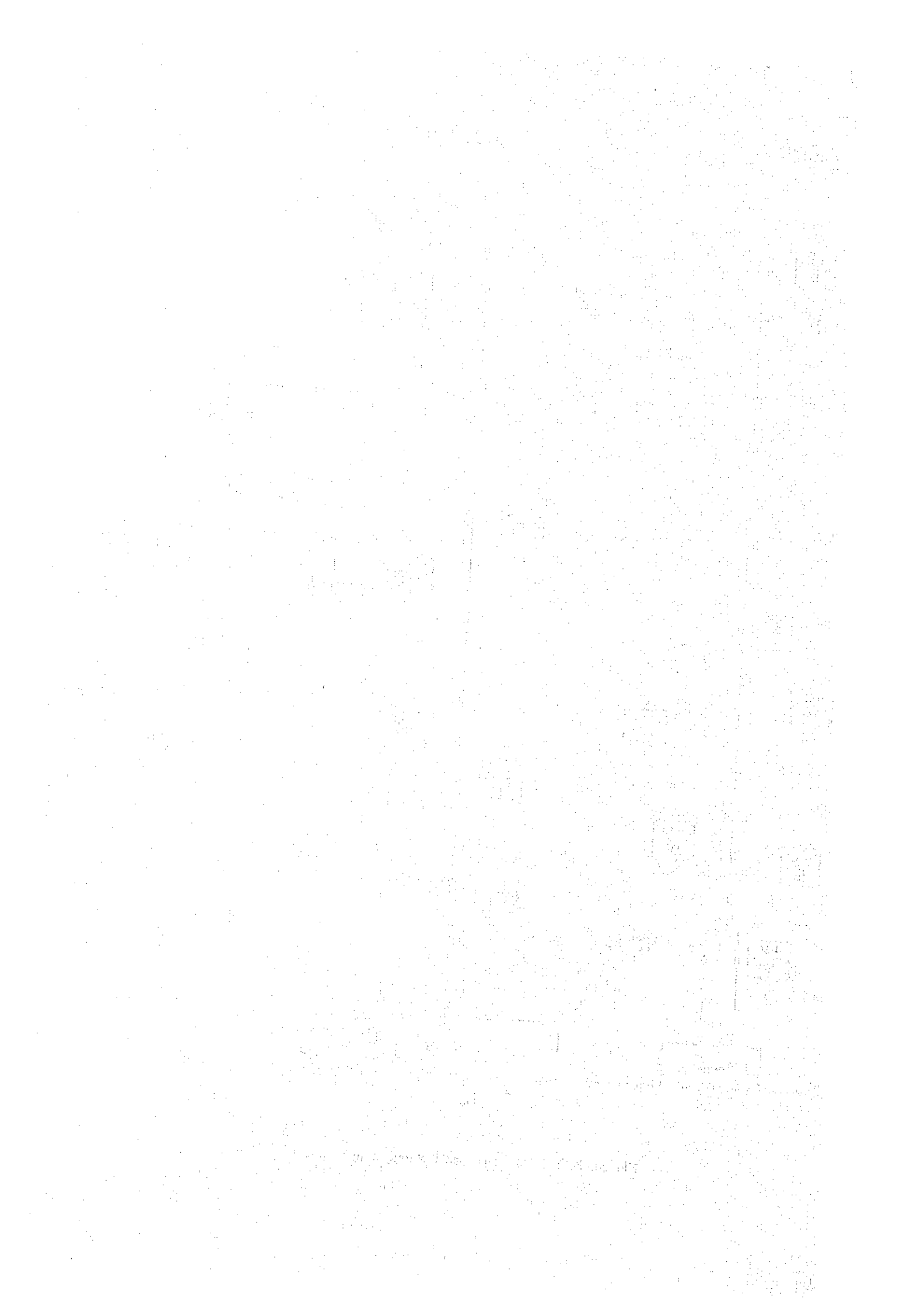


Fig. S5.3.3 SS Inflow Load in Normal Time

1988. 7



PIRAYU B.

YUQUYRY B.

△ Survey Point at River

$Q(m^3/S)$
 $L(kg/d)$ TP

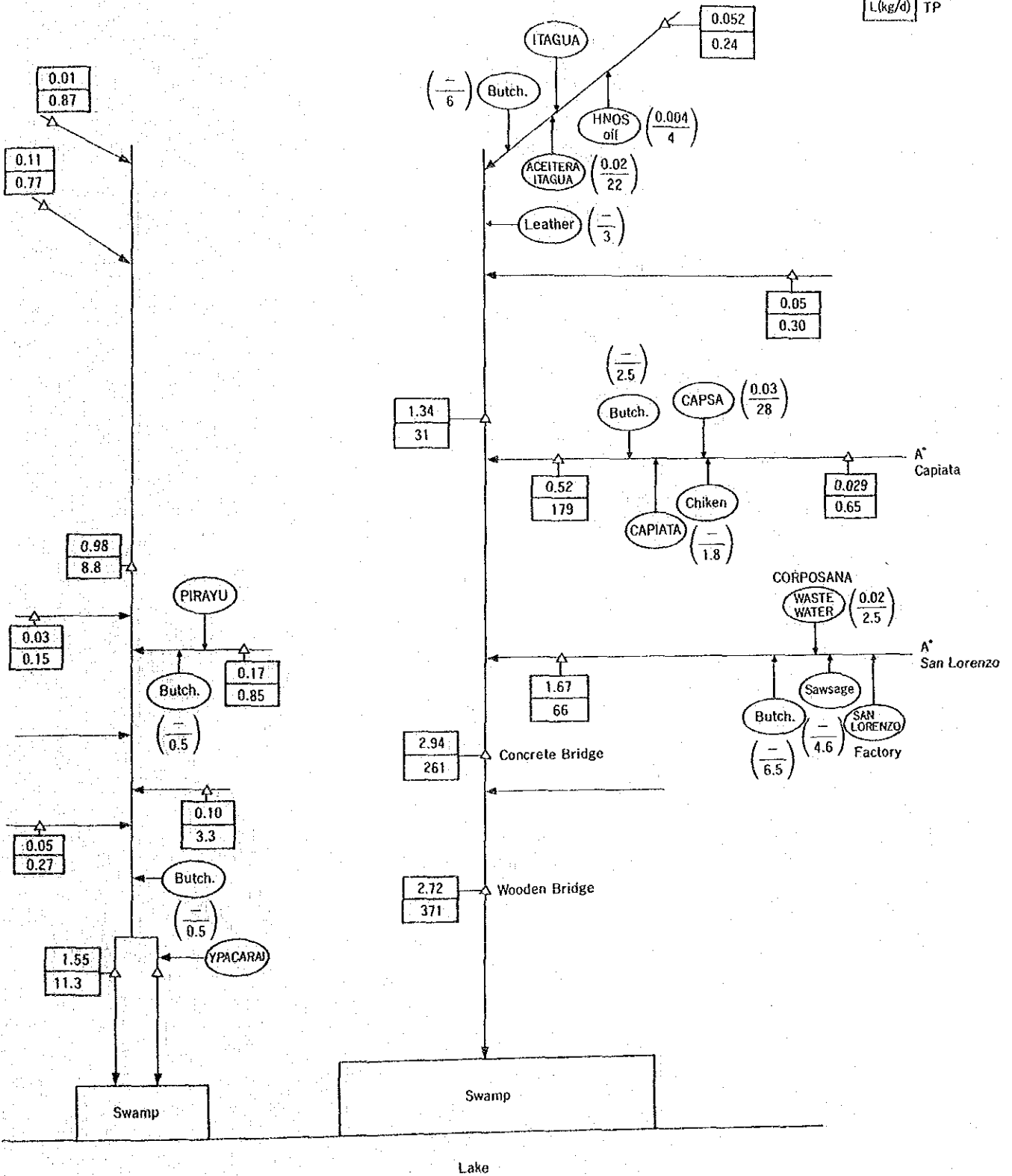
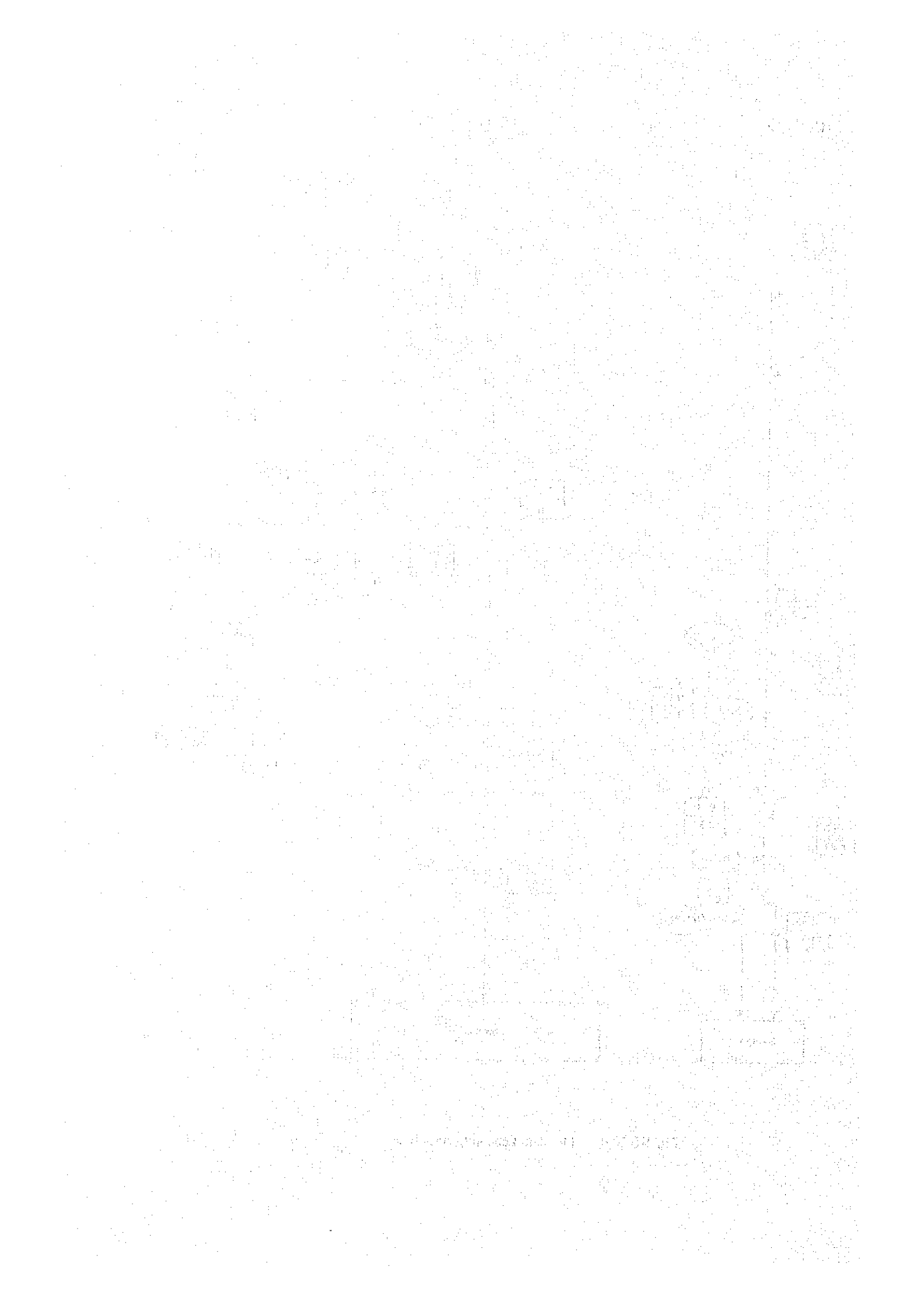


Fig. S5.3.4 TP Inflow Load in Normal Time

1988. 7



PIRAYU B.

YUQUYRY B.

△ Survey Point at River

Q(m³/s)
L(kg/d) TN

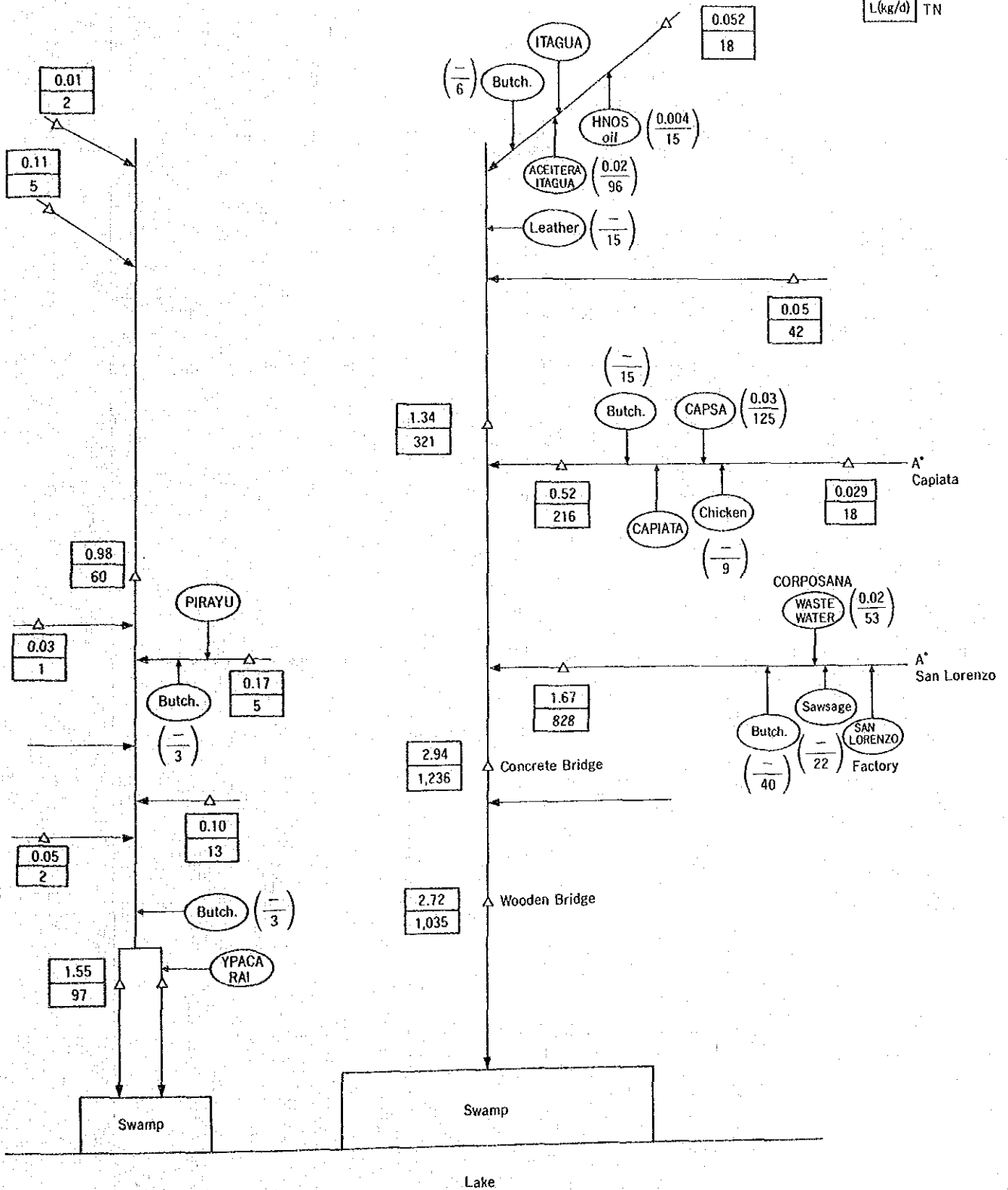
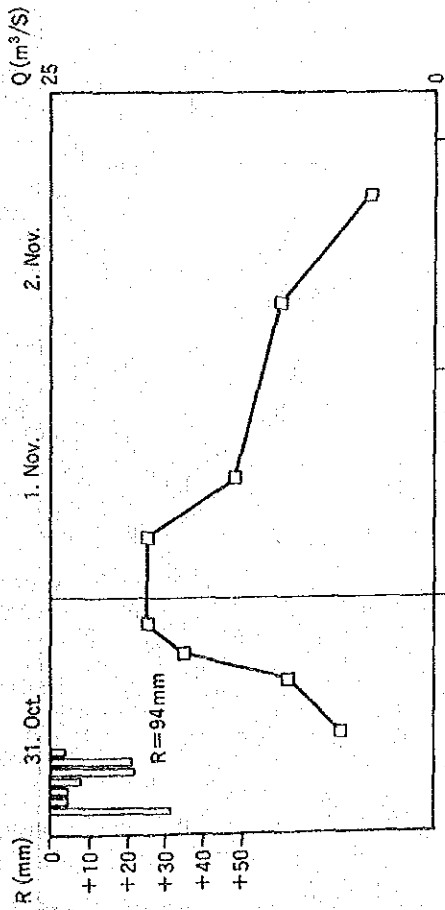


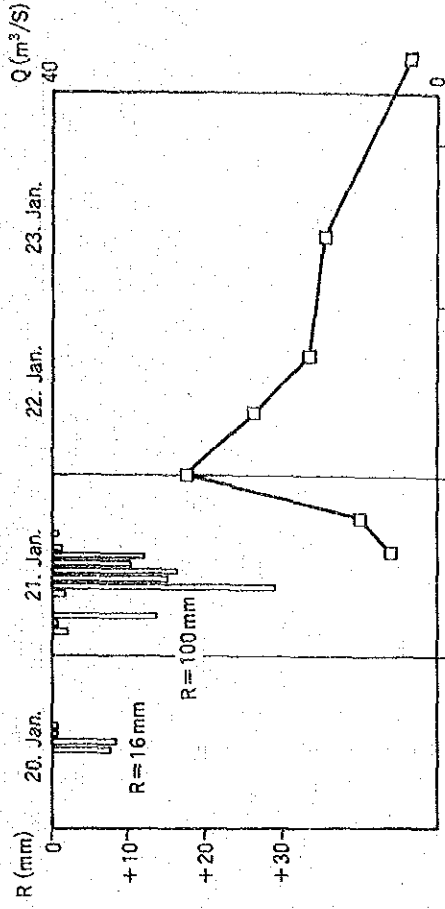
Fig S5.3.5 TN Inflow Load in Normal Time

1988. 7

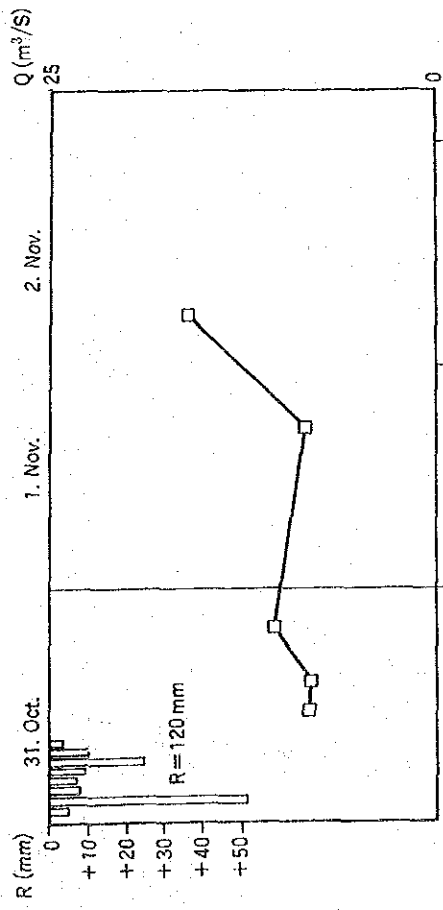
YUQUYRY, B. 1989. 10. 31



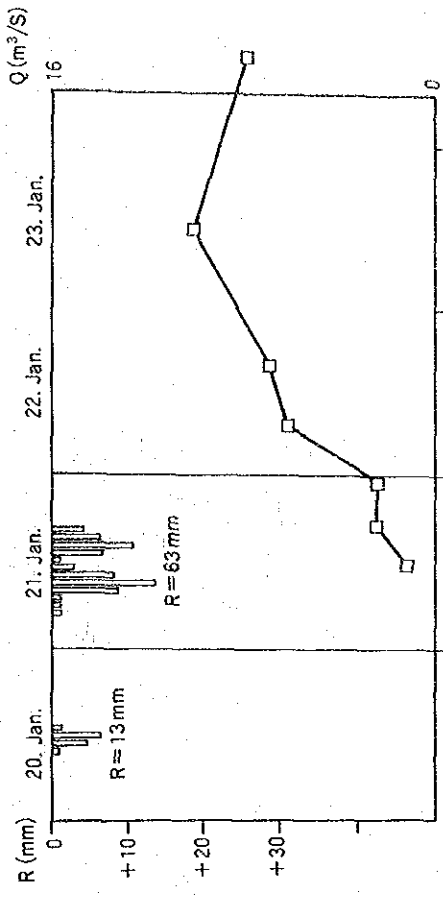
YUQUYRY, B. 1989. 1. 20~21



PIRAYU, B. 1989. 10. 31



PIRAYU, B. 1989. 1. 20~21



* Remarks
Precipitation Data is Revised by Tiesen Method

Fig.S5.3.6Hyetograph & Hydrograph at The Survey Point of Inflow River in Flood Time

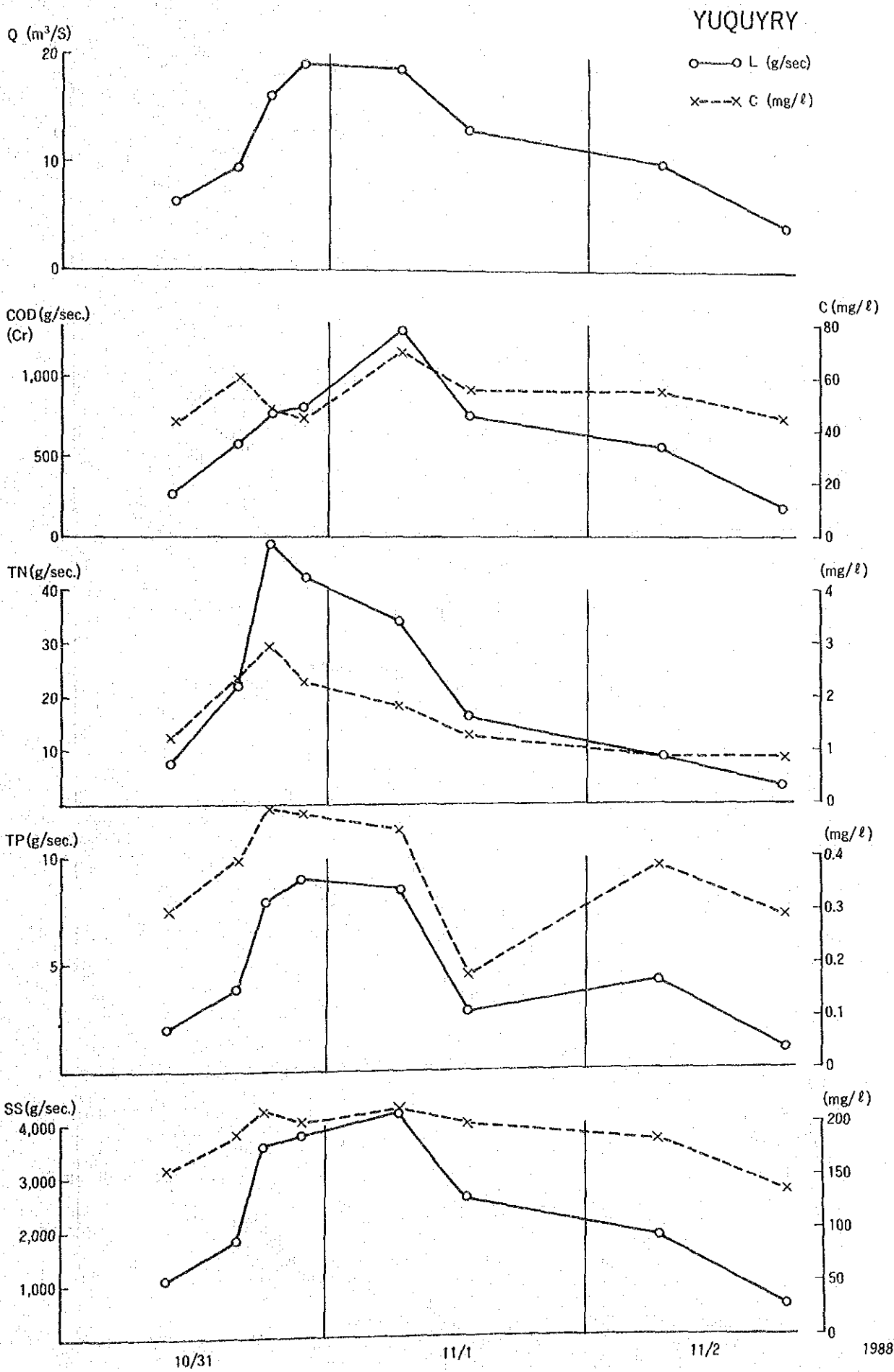
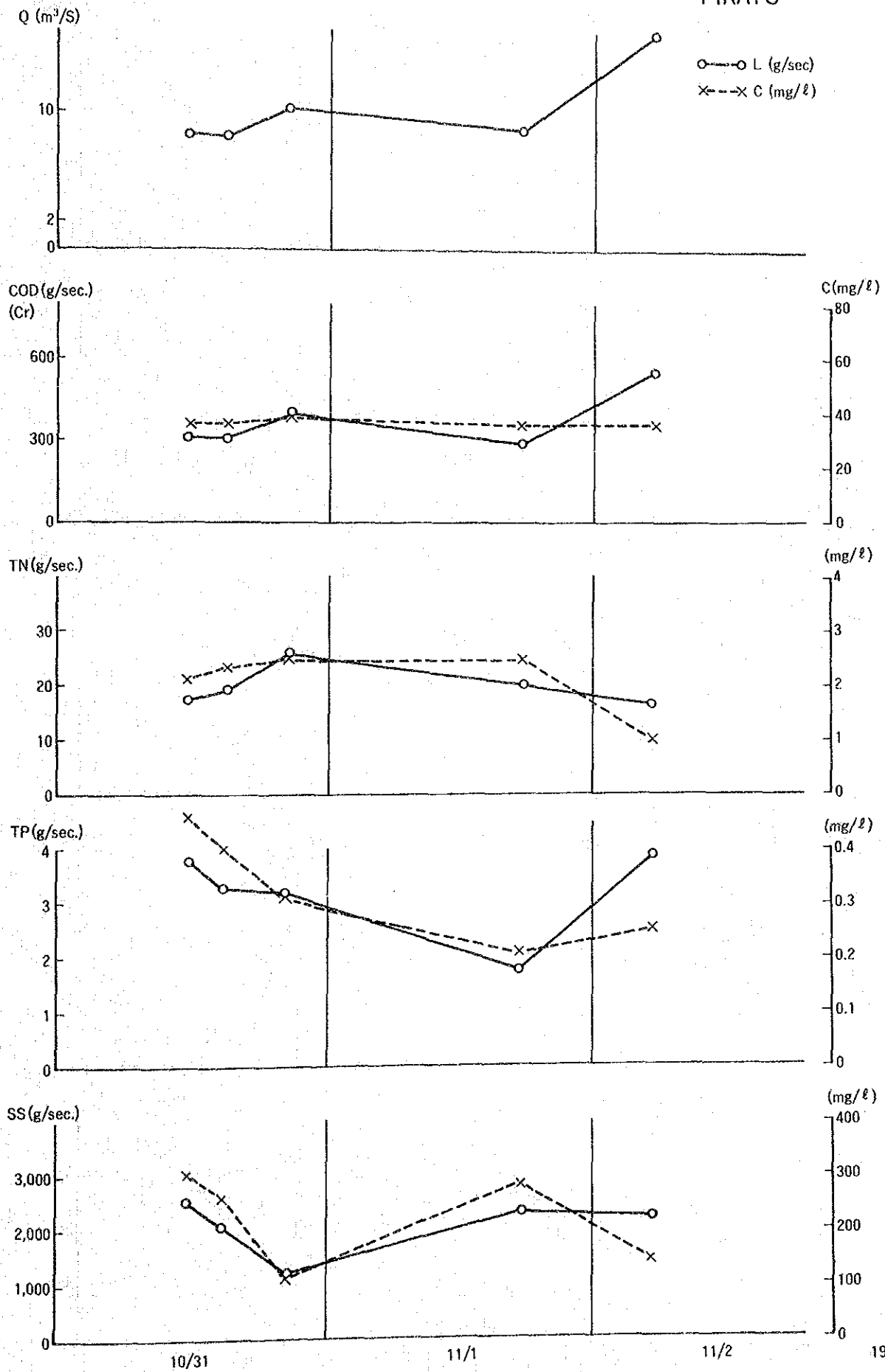


Fig. S5.3.7 Inflow Load in Flood Time (1)

1988

PIRAYU



1988

Fig. 55.3.8 Inflow Load in Flood Time (2)

YUQUYRY

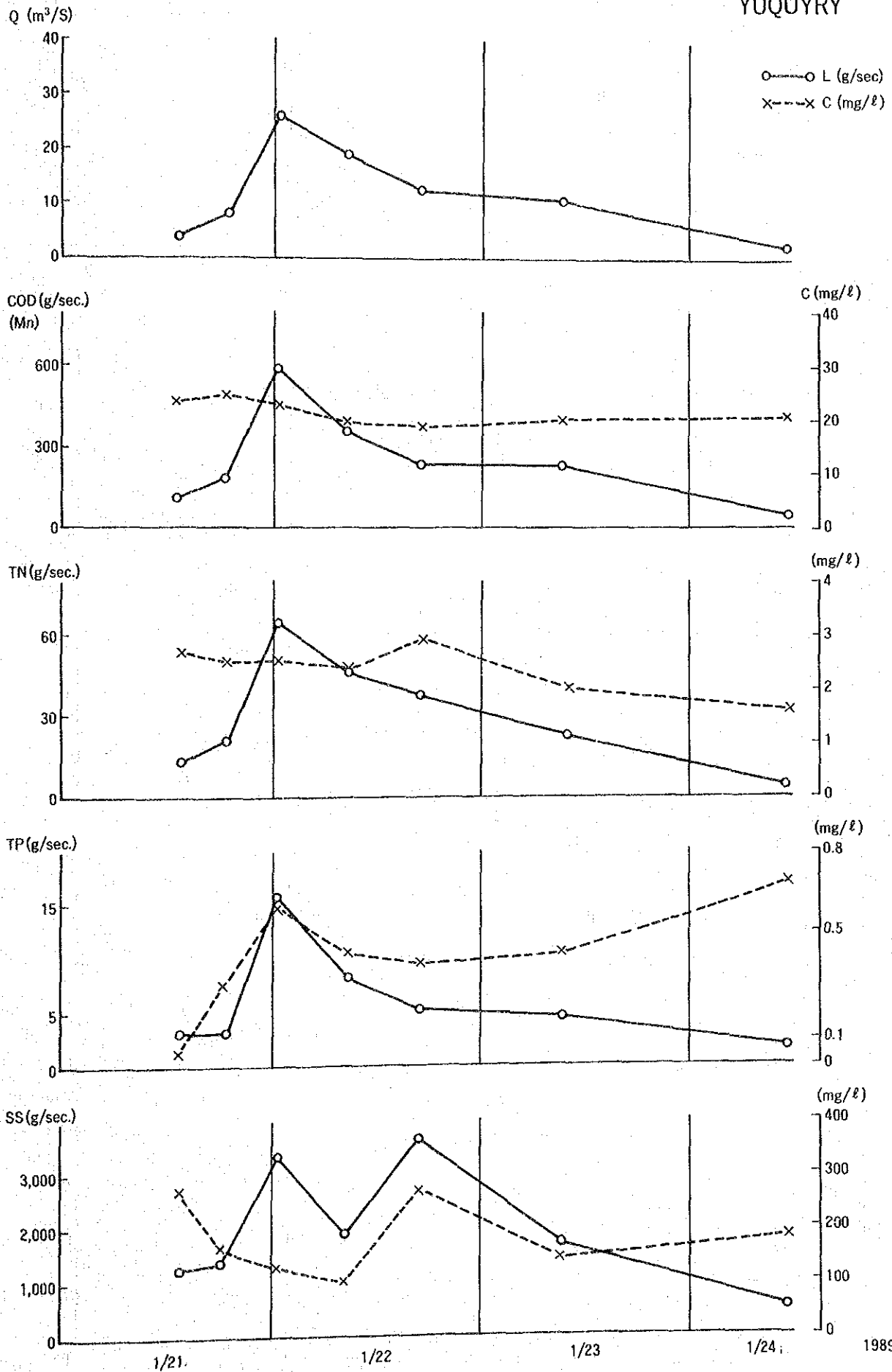


Fig. S5.3.9 Inflow Load in Flood Time (3)

PIRAYU

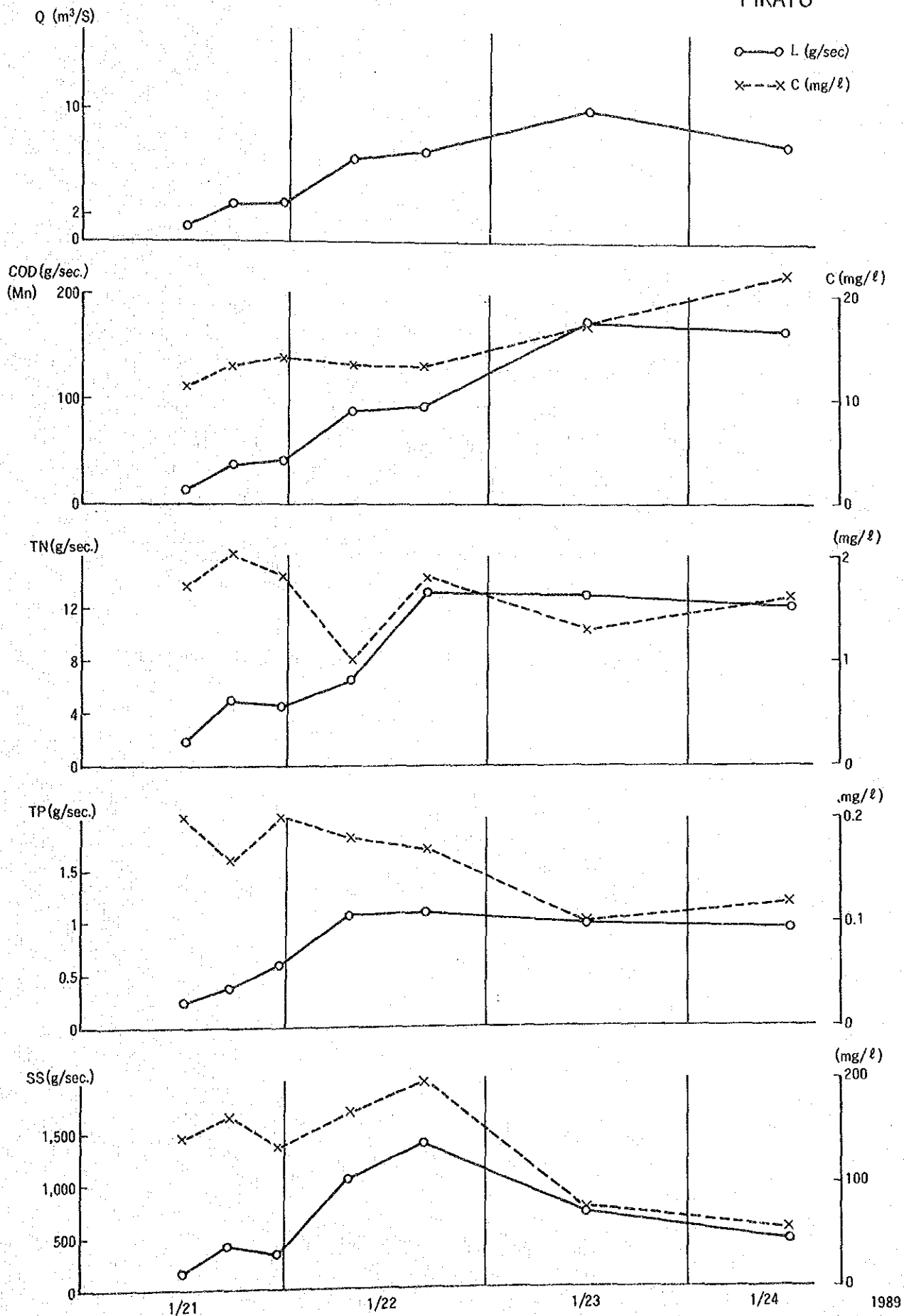


Fig. S5.3.10 Inflow Load in Flood Time (4)

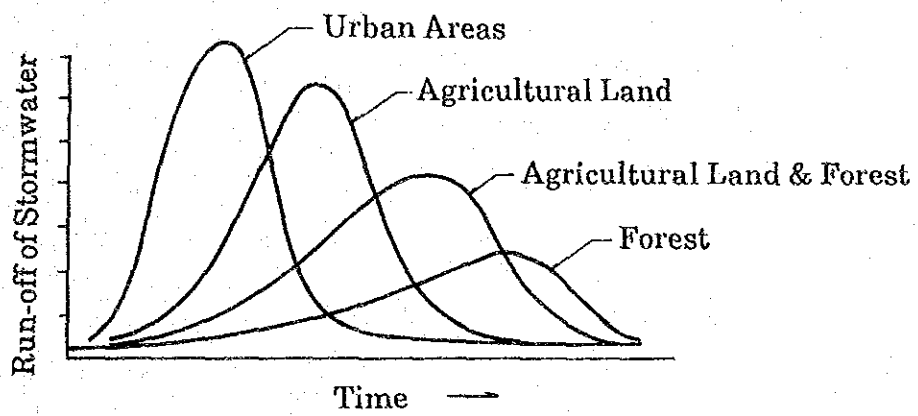
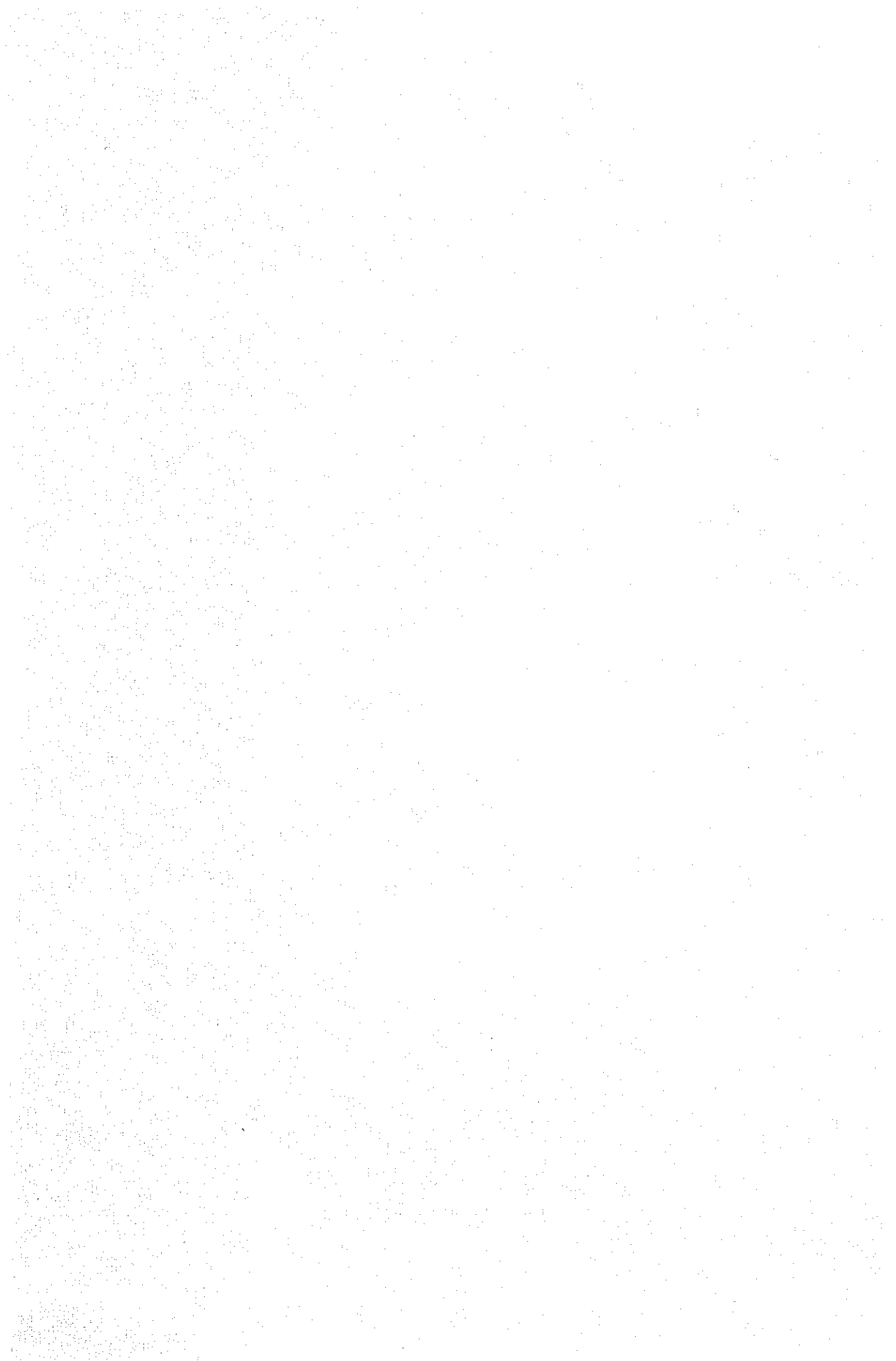


Fig. S5.A.1 Rainfall Runoff according to Types of Land use



JICA